DISCLAIMER

This draft chapter is a work in progress and is being provided to the public for information purposes only. Because it is a work in progress, there are parts that are either missing or will be revised, and the page numbers will change. Permission to cite any part of this work must be obtained from the prime author. The final version of this chapter will be published in Volume 10 of the *SeaWiFS Postlaunch Technical Report Series*.

Chapter 3

Changes Made in the Operational SeaWiFS Processing

Wayne D. Robinson and G. Michael Schmidt

SAIC General Sciences Corporation, Beltsville, Maryland

Charles R. McClain

NASA Goddard Space Flight Center, Greenbelt, Maryland

P. Jeremy Werdell

Science Systems and Applications Incorporated, Lanham, Maryland

Abstract

This chapter discusses the major changes made in the SeaWiFS processing for the second reprocessing of August 1998 and the third reprocessing in May 2000. Each major change in the processing programs and tables is presented with a description of the effects of the change. For the second reprocessing, a review of the major changes to the data is presented using a eight-day period of data as an example. The effect of the changes for the third reprocessing are also examined and compared to the results of the second reprocessing using two eight-day periods of data. The changes have increased the usefulness of the data in both oceanographic and atmospheric applications.

3.1 INTRODUCTION

This chapter discusses the major changes made in the SeaWiFS level-1, -2, and -3 processing which led to the third reprocessing. Ever since the first SeaWiFS reprocessing of 2 January 1998, the SeaWiFS Project personnel have been evaluating the results of the processing and discovered many problems and improvements. Some problems were fixed in the operational software, but many improvements which required recalibration could not be installed without initiating a complete reprocessing. These changes were accumulated for a period of approximately six months before applying them to all the data in the second reprocessing. During this period, significant changes in the calibration of SeaWiFS bands 7 and 8 (Eplee and McClain 2000a) made it imperative to include the calibration and other changes into the operational processing promptly so that the quality of the data could be maintained.

The second reprocessing started on 14 August 1998. At that time, the new software was used to reprocess all of the data collected from the start of the mission and to process the real-time data as it arrived. Since the second reprocessing, several minor enhancements and repairs were made to the operational processing software.

Several remaining problems, which were recognized after the second reprocessing, were investigated extensively; many improvements were developed to make the resulting data more useful and to broaden the product suite. All these changes were incorporated in the third reprocessing, which occurred in May 2000.

The next section discusses the major changes made in the software and tables for the second reprocessing, and the impact of those changes on the products. A brief summary of the combined effect of those changes is discussed in Sect. 3.2.4. The major changes included in the third reprocessing are presented in Sect. 3.3. Section 3.3.6 is an analysis of the changes in the derived products from the second to the third reprocessings, followed by the conclusion which summarizes these changes and lists future improvements.

3.2 THE SECOND REPROCESSING

In the approximately six months between the first and second SeaWiFS reprocessings, many changes were made in the level-2 and -3 processing software. The most significant changes in that period are shown in Table 1 and are discussed briefly here. The details of changes related to the calibration, atmospheric correction, and the new chlorophyll algorithm are discussed elsewhere in this three volume set, Volumes 9–11, of the *SeaWiFS Postlaunch Technical Report Series*.

3.2.1 Calibration Related Changes

In the period leading up to the second reprocessing, the calibration of the SeaWiFS instrument became more rigor-

Table 1. Major changes in the second reprocessing.

Change	*Observable Effect*
Calibration:	
Prelaunch Calibration Change	None
Time dependence of bands 7, 8	Better temporal stability
Revised vicarious calibration	None
Atmospheric Correction:	
New transmittance tables	Remove L_{WN} as f (scan angle)
Wider range of aerosol models	Reduce number of points outside model range
Other:	
Updated coefficients for chlorophyll algorithm	Increase low chlorophyll and decrease high chlorophyll
Added test for high reflectance ratios	Removal of spurious chlorophyll
Tests to decrease chlorophyll speckles	Some reduction on speckles
Improved L_{WN}computation	$< 1\%$ change in L_{WN}
Noise resistant dark count	No striping in the data
Improved solar radiance computation	None
More accurate anchor point grid	None
Reduce whitecap radiance	Reduction in data loss
Bin higher chlorophyll	Retain larger chlorophyll range
Write out actual ϵ values	Better diagnostics on ϵ values

ous, with a more detailed band 7 calibration and better detector characterization. Three calibration related changes are presented here.

3.2.1.1 Prelaunch Calibration Changes

The first reprocessing was conducted using a preliminary set of SeaWiFS calibration values determined in January and April 1997. When an analysis of the calibration data was completed (Johnson et al. 1999), the calibration was modified to include these updates and this calibration was used for the second reprocessing. The changes in the total radiances was less than 0.5%.

3.2.1.2 Time Dependent Calibration

In 1998, the time series of solar and lunar calibration measurements, which began in September 1997, showed that the radiometric response of bands 7 and 8 was changing as a function of time. The greatest change occurred in band 8, amounting to a 4–5% drop in the total radiances. The calibration table used during the second reprocessing was adjusted to compensate for these changes and was updated as needed thereafter in the operational processing. A detailed discussion of the calibration is in Eplee and Barnes (2000a and 2000b).

3.2.1.3 Revised Vicarious Calibration

Improvements were made in the vicarious calibration of band 7 relative to band 8, and for bands 1– 6. Details of the vicarious calibrations are discussed in Robinson and Wang (2000) and Eplee and McClain (2000a), but a short summary is presented here.

The band 7 vicarious calibration was accomplished by adjusting the band 7 gain factor until the ratio of the single-scattering aerosol radiances in bands 7 and 8 (referred to as the ϵ value), matched the expected ratio over open ocean. This process was applied to a limited number of sites in the first reprocessing. The current band 7 calibration extends and improves this procedure by selecting open-ocean sites near Hawaii, evaluating the gain using the time series of SeaWiFS LAC data supporting the MOBY site, and using strict screening procedures for data quality.

The calibration for bands 1–6 was derived by adjusting the gain factors for each band until the water-leaving radiances in those bands matched those measured by MOBY. In the second reprocessing, the calibration was improved with more MOBY observations.

3.2.2 Atmospheric Correction Changes

Wang (2000) presents a more detailed description of the changes made in the atmospheric correction. Two major changes are briefly described here.

3.2.2.1 New Transmittance Tables

The transmittance tables were corrected to include the Fresnel reflectivity of the air–water interface. The introduction of this correction removed a small scan-angle dependence in the normalized water-leaving radiance (L_{WN}). The changes reduced the L_{WN} in bands 1–5 by 2% at the center of the scan. At the edge of the SeaWiFS GAC scan, the L_{WN} was reduced by about 5% and at the edge of a LAC or high resolution picture transmission (HRPT) scan, the reduction was about 10%.

3.2.2.2 Wider Range of Aerosol Models

In the process of performing the atmospheric correction, the level-2 processing determines the atmospheric model that most matches the ϵ value, or ratio of aerosol radiances in bands 7 and 8. For about 40% of the points processed in the first reprocessing, the ϵ value was below the lowest ϵ value of the available models. In these cases, the atmospheric correction was forced to use the model with the lowest ϵ value to derive the aerosol radiances for the other bands. Although this model was the best available, it is not as correct as a model that would fit the observed ϵ value.

In the second reprocessing, the model suite was expanded to include oceanic aerosol models which contain lower ϵ values. The new atmospheric model suite reduced the occurrence of points below the model range from 40% to about 20%.

3.2.3 Other Changes

Other changes made to the SeaWiFS processing affect both the level-2 and -3 algorithms. The changes correct minor problems, improve algorithms, or reduce noise in the products.

3.2.3.1 Improved Chlorophyll a Algorithm

The relationship between L_{WN} and chlorophyll was updated with additional *in situ* observations (Maritorena and O'Reilly 2000), resulting in a new set of coefficients for the equation relating the ratio of the L_{WN} to chlorophyll in the 490 and 555 nm bands. The new relationship increased chlorophyll values that are less than .03 mg m^{-3} and decreased chlorophyll values that are greater than 1 mg m^{-3}.

It was found that under conditions of very large reflectance ratios, (values greater than 10), the chlorophyll algorithm could return reasonable chlorophyll values. The chlorophyll failure flag was set in these instances so that these values would not be binned. A similar treatment was applied in the third reprocessing.

3.2.3.2 Decreased Chlorophyll a "Speckling"

The SeaWiFS level-2 and -3 binned data contained isolated pixels with relatively high chlorophyll values in fields with otherwise low chlorophyll values. Frequently, these *speckles* were near cloud edge not masked as "cloud". Methods of removing these points, such as, decreasing the band 8 albedo threshold for cloud masking or expanding the stray light distance, caused a great number of good data points to be masked in the process of removing a few bad points.

An alternate method was used that masked many occurrences of speckles without masking out good data. A mask was applied to pixels in which any of the bands 1–8 had zero or negative values after their radiances were corrected to remove the effects of ozone absorption, whitecap radiance, and Rayleigh radiance. The masked points were assigned the atmospheric correction failure flag (which is usually a mask). The new test reduced occurrences of speckles but did not eliminate it. This test also revealed cases where the whitecap correction was too large (Sect. 3.2.3.7).

3.2.3.3 Improved L_{WN} Computation

The L_W normalization step of the level-2 processing was improved to include a more realistic atmospheric attenuation than the attenuation used in the first reprocessing. In the first reprocessing, the normalization only used the Rayleigh scattering and ozone absorption to correct for the attenuation in the path from the sun to the surface. For the second reprocessing, the effect of aerosol scattering was included. The effect was to slightly reduce the L_{WN} values in bands 1–5 by less than 1%.

3.2.3.4 Noise Resistant Dark Count Calculation

Striping was noticed in the radiance data, the cause for which was traced to the *dark count* calculation used in the calibration. (The dark count is the digital count value measured by the detectors when looking at a dark surface and thus, represents a zero value in the calibration. The dark count is collected for every scan line of data, has a nominal value of 20 counts, and remains virtually constant throughout an entire data pass.) In some of the data, the dark count had a tendency to change by one digital count from one line to the next (or jitter). This jitter caused the striping in the radiances from line to line. In order to remove the jitter, the dark counts were averaged to estimate a dark count offset for the entire pass. With the onset of data encryption, a number of dark count values that were very different from the standard values from undecrypted lines, were included in the algorithm that computes the average dark count. The resulting dark count average occasionally produced badly calibrated radiances and caused the entire scene to have radically different normalized water-leaving radiances than expected.

The dark count calculation was improved using the following two steps:

1) Remove any dark count values from consideration that are less than 5 or greater than 35 counts, and
2) Take the median value as the dark count for the pass.

The improvements were especially helpful for HRPT data, which frequently has trouble with noise at the start and end of a pass. On occasion, it also helped improve the quality of GAC and LAC data.

3.2.3.5 Improved Solar Radiance Computation

A 0.1% error in the value of the correction in the solar irradiance, as a function of the time of year, was discovered in the level-2 processing. The correction was improved to

reduce this error to 0.001%. A 0.1% error in the solar irradiance roughly translates to approximately a 1.0% error in the L_{WN} values.

3.2.3.6 More Accurate Anchor Point Grid

In order to speed up calculations of parameters, such as, the ancillary data values and Rayleigh radiances, the level-2 processing program used a set of anchor points at which these quantities were computed exactly. The values of the ancillary data at other points were computed by interpolating the anchor point data to that location. For the first reprocessing, the anchor point separation was eight pixels for LAC and HRPT data and two pixels for GAC pixels. In some cases, the departure of the interpolated Rayleigh values from the exact values was significant, e.g., as great as $0.015\,\mathrm{mW\,cm^{-2}\,\mu m^{-1}\,sr^{-1}}$ in the Rayleigh radiance at 443 nm, which roughly translates to a 1% error in the L_{WN}. On average, this error was less than $0.002\,\mathrm{mW\,cm^{-2}\,\mu m^{-1}\,sr^{-1}}$. This error was reduced to less than $0.004\,\mathrm{mW\,cm^{-2}\,\mu m^{-1}\,sr^{-1}}$ in the second reprocessing by reducing the anchor point separation by a factor of 2 (one pixel in GAC and four pixels in LAC and HRPT) to improve the accuracy of the Rayleigh and other ancillary data used. (Note that in the third reprocessing, all calculations are done at every point).

3.2.3.7 Reduced Whitecap Radiance Effect

Several instances have occurred where a region of ocean was cloud-free, but was masked out as an atmospheric correction failure because the ozone, whitecap, and Rayleigh-corrected radiances in some bands were negative (a mask condition intended to reduce speckles in the chlorophyll concentration). It was discovered that in very clear regions with high wind speeds (around $15\,\mathrm{m\,s^{-1}}$), the whitecap correction was so large in bands 7 and 8 that the remaining radiance was smaller than the Rayleigh radiance and caused the region to be masked. A 75% reduction in the whitecap correction was implemented to solve this problem. In discussions with H. Gordon, this reduction factor seemed reasonable. Also, studies of the whitecap contributions (Gordon and Wang 1994) show a great amount of variability in the whitecap radiance under high wind conditions. The main effect of this change in the whitecap correction was to allow previously overcorrected and masked areas to be processed.

3.2.3.8 Binning of Higher Chlorophyll Values

It was noticed that in the process of binning the level-2 data, a large amount of high chlorophyll data was being excluded. The primary reason for this was that many pixels had a valid chlorophyll value (i.e., the L_{WN} in bands 3 and 5 were positive), but the L_{WN} values in bands 1 or 2 was negative. In the first reprocessing, the presence of negative L_{WN} values in a measurement was one of the exclusion conditions for the binning.

In order to bin more of these excluded chlorophyll values, a number of changes were made in the level-2 and -3 programs. First, the level-2 program was modified to output the actual negative water-leaving radiances that were derived instead of a -1.0 value. This allows an investigator to get a better idea of how large the negative L_{WN} values are. The binning routine was modified to bin pixels that have negative L_{WN} values in them, but to bin them as zeros. In addition, the chlorophyll algorithm failure flag (`CHLOR1`) was added as a binning flag so that points which had a chlorophyll algorithm failure (band 3 or 5 where L_{WN} is less than 0 or where chlorophyll values are greater than 64) would not get binned. This set of changes restored much of the high chlorophyll data that was previously excluded.

3.2.3.9 Actual Epsilon Values

In the first reprocessing, the aerosol correction algorithm in the level-2 processing code reported the ϵ value for the nearest aerosol model in cases where the derived ϵ value was actually outside of the model range. This caused some uncertainty in the actual value of ϵ, and it also tainted some calculations that used the average value of ϵ.

The aerosol correction algorithm was modified to report and store the actual ϵ value computed. This ϵ value was also used in the aerosol calculations.

3.2.4 Second Reprocessing Analysis

In many cases, L_{WN} value changes brought about by level-2 processing algorithm changes were compensated for when the vicarious calibration was applied. The only way to understand the effects of all the changes was to consider them after this calibration was implemented. The cumulative effect of all the above changes is discussed in this section. The effect of all the changes to the processing is studied using a sample of typical SeaWiFS data.

3.2.4.1 Chlorophyll a *Changes*

Figure 1 shows the global frequency distribution of chlorophyll resulting from processing using the first reprocessing (dotted line) and the second reprocessing (solid line) for an eight day period from 14–21 March 1998. The second reprocessing chlorophyll values are higher in open ocean regions, such as the South Pacific and Atlantic. Large regions that previously had chlorophyll concentrations at the lowest value of $0.01\,\mathrm{mg\,m^{-3}}$ with the first reprocessing, had their values increase to around $0.03\,\mathrm{mg\,m^{-3}}$ with the second reprocessing. This was mainly the result of the new chlorophyll algorithm, although some contribution resulted from the new transmittance tables and calibration. The increased chlorophyll values observed in the second reprocessing agreed better with observations of the lowest chlorophyll, i.e., values of $0.01\,\mathrm{mg\,m^{-3}}$ are rarely observed. The distribution of chlorophyll was raised significantly in

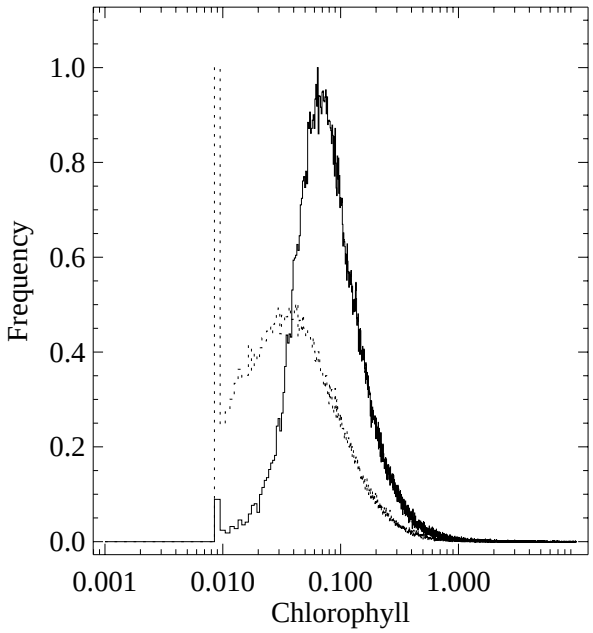

Fig. 1. The SeaWiFS level-3 global chlorophyll *a* frequency distribution for the eight day period of 14–21 March 1998 using the processing algorithms for the first reprocessing (dotted curve) and for the second reprocessing (solid curve).

the second reprocessing. The peak value of chlorophyll increased from 0.02–0.05 mg m^{-3} and far fewer points had the lowest chlorophyll value of 0.01 mg m^{-3}. A number of observations still appeared to go below the lower limit of 0.01 mg m^{-3} in the second reprocessing.

Another aspect of the second reprocessing was that the total number of filled bins in the time binned product increased by 5%. Many of the new points were in high chlorophyll areas—a direct result of the new binning strategy that retained a greater number of high chlorophyll values (Sect. 3.2.3.8). Many of the new points were in coastal regions and in the Baltic Sea.

The second reprocessing significantly reduced the values of the highest chlorophyll (another direct effect of the new chlorophyll algorithm). Chlorophyll values near many coastal areas showed decreases up to 30%. The second reprocessing changes also resulted in an increase of the L_{WN} values in bands 3 or 5 so that chlorophyll values could be determined in more coastal areas.

Both the increase in very low chlorophyll and the decrease in high chlorophyll were positive changes that occurred in the new processing.

3.2.4.2 Water-Leaving Radiance Changes

An analysis of the global distribution of L_{WN} showed a general increase in the L_{WN} values with the second reprocessing. For instance, the mean L_{WN} at 555 nm was increased by 0.06 from 0.26–0.32. The new mode of 0.27 (versus 0.21 in the first reprocessing) had better agreement with the MOBY-derived clear-water L_{WN} value of 0.254 (Eplee and McClain 2000b).

In the blue bands, considerably less change was observed in the L_{WN} distribution. The mean L_{WN} at 412 nm increased only slightly from 1.53–1.56. In some isolated regions along the coast, L_{WN} actually decreased somewhat. The decreases may have been due to the inclusion of zero values of L_{WN} in the binning algorithm (Sect. 3.2.3.8). It was hoped that the second reprocessing changes would reduce the number of negative L_{WN} values in bands 1 and 2. Although L_{WN} increased overall, there were still problems. The next section looks at the distribution of negative L_{WN} values in more detail.

3.2.4.3 Distribution of Negative L_{WN} Values

The occurrence of negative L_{WN} values, especially in bands 1 and 2, has always been a problem in the SeaWiFS processing. Because the second reprocessing retained the *actual* values of the negative normalized water-leaving radiance, instead of setting them to zero, it was possible to look at the distribution of the negative L_{WN} values.

The geographic distribution of negative L_{WN} values in the 412 nm band is presented in Fig. 2 for all level-2 data that was not masked by the level-2 flag conditions (atmospheric correction failure, land, high radiances, glint and clouds) and stray light, in the eight day period from 12–19 July 1998. Regions that had occurrences of negative L_{WN} values greater than 50% are shaded black.

The negative L_{WN} distribution shows the largest problems to be along the coast and in the extreme northern and southern latitude regions. The coastal waters have higher chlorophyll concentrations and are the most likely to have

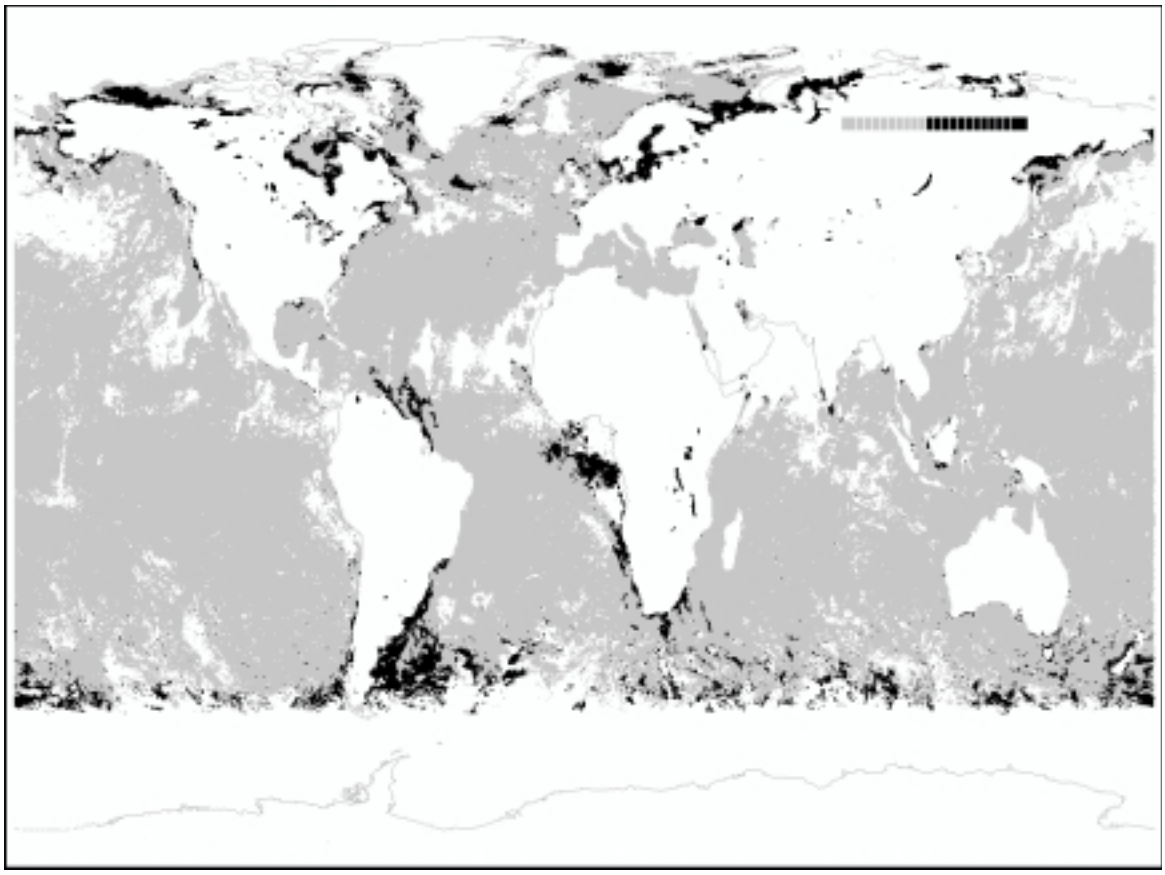

Fig. 2. Percentage of occurrence of negative L_{WN} values at 412 nm for the eight day period from 12–19 July 1998. This image was generated using the second reprocessing algorithms and uses data that is excluded by the standard level-2 processing: atmospheric correction algorithm failure, land, sun glint, high total radiance, and clouds. In addition, stray light pixels are excluded. White areas indicate no data—continental land masses make up a great part of this region—while light gray indicates data present with occurrences of negative L_{WN} values of less than 50%. The regions shaded black all have more than 50% occurrence of negative L_{WN} values, indicating areas that are severely affected by negative L_{WN}.

problems with turbid water or dust in the atmosphere affecting the aerosol correction. The non-coastal areas in the Southern Ocean (and to some degree in the extreme North Atlantic) with negative L_{WN} values also have relatively high chlorophyll values but should not have other coastal problems, such as continental aerosols. The amount of negative L_{WN} in these areas decreases as wavelength increases (not shown) and was fairly negligible at, and above, the 490 nm wavelength.

The distribution of negative L_{WN} values in higher latitude regions suggests that the problem may be related to poor treatment of the atmospheric corrections at high solar zenith angles. The 12–19 July data was taken when the sun was at a latitude of 20°N. In that data (Fig. 2), the significant increase in negative L_{WN} values appeared to occur at 40°S and possibly 80°N, which translates into solar zenith angles of around 60°. When the percentage of negative L_{WN} values at 412 nm is plotted as a function of solar zenith angle (Sect. 3.3.6.2), a large increase in the percentage of negative L_{WN} values is seen at a solar zenith angle of 60°. Similar behavior occurred for a period in January 1998 (not shown). This behavior may indicate a breakdown in the plane parallel atmosphere assumption used to derive aerosol model behavior (Ding and Gordon 1994). This possibility was investigated further in preparation for the third reprocessing.

An additional occurrence of negative L_{WN} values was scattered throughout the open ocean areas, but unlike the coastal areas, the frequency of negative L_{WN} values in these areas was relatively small. In the 510 and 555 nm bands (not shown), the distribution of open ocean negative L_{WN} values increased somewhat. This effect was found to mainly be due to the influence of cloud shadows, noise, and stray light on the radiances. When the binning flags (which include masks for low $L_{WN}(555)$ values) were included, this problem was almost entirely removed in band 1 and the other bands.

The binning masks appeared to aid in removing some of the negative L_{WN} values, but large coastal areas remained severely affected by this problem.

3.3 THE THIRD REPROCESSING

The second reprocessing was able to improve on the algorithms used to perform the calibration and processing of the SeaWiFS data to water-leaving radiances and derived geophysical quantities. It also left many important questions to be resolved. The most important concern was to determine what was causing the large number of negative L_{WN} values in coastal areas. The effort to understand and solve this problem and the algorithms chosen for the third reprocessing are presented here.

In the period leading up to the third reprocessing, a number of improvements were also made in the calibration and the atmospheric correction algorithms. Calibration improvements were possible with more measurements which led to greater understanding of the instrument performance.

Another large change was the migration of the level-2 processing algorithms to a new program, `MSl12`, which greatly improved the ease of use and the incorporation of new algorithms. `MSl12` allowed the selection of many more intermediate results and final parameters. With this migration, several basic changes were made in the default operational products and in the available flags. The major operational changes are summarized in Table 2 and brief descriptions of the changes are presented in the following sections, as well as, the results of the third reprocessing (Sect. 3.3.6).

3.3.1 Calibration Related Changes

The changes to the calibration included the routine characterization of the detector degradation, as well as, a better understanding of instrument behavior. Increased use of the SeaWiFS data for cloud and aerosol studies revealed other calibration problems, which were solved for the third reprocessing.

3.3.1.1 Expanded Time-Dependent Calibration

The SeaWiFS CVT has updated the time-dependent calibration as new lunar calibration measurements become available each month. Previously (Sect. 3.2.1.2), a time dependence could only be seen occurring in the two near-infrared bands at 765 and 865 nm. A longer time period of observations, and more accurate treatment of the radiance model of the moon, have made it possible to detect and make a correction for time-dependent changes in radiometric response in many of the remaining bands (Eplee and Barnes 2000a). The largest change now seen in bands 7 and 8 (765 and 865 nm) are a 2% and 10% decrease, respectively, while bands 1 and 6 (412 and 670 nm) show 1% decreases, and bands 2 and 5 (443 and 555 nm) show 0.5% decreases. Bands 3 and 4 (490 and 510 nm) are assumed to have no change. The SeaWiFS calibration now contains time-dependent corrections for all these bands.

3.3.1.2 Bilinear Gain Adjustments

During work to derive a measure of absorbing aerosols (Hsu et al. 2000 and Fukushima et al. 1999), it was determined that there was a discontinuity in the frequency distribution of total radiances which occurred at the region where the instrument gain changed to a lower sensitivity (the *knee point*). This indicated that the relation between raw satellite counts and total radiance was incorrect for radiance values above the knee. The radiance value at which this discontinuity occurred was above the range where most ocean color processing is performed and, therefore, has no effect. It does have an effect on the analysis of dense aerosols, absorbing aerosols, and clouds. It was assumed that the laboratory setting of the knee point was either incorrect or had shifted.

The knee points were redetermined by finding the settings that minimized the discontinuity in the frequency distributions of the total radiances (Eplee 2000). The implementation of this change reduced the radiances above the knee by 0.8% on average, and increased the radiance below the knee by about 0.1%.

3.3.1.3 Revised Vicarious Calibration

The calibration of bands 1–7 was performed for the third reprocessing in much the same way as it was done for the second reprocessing (Sect. 3.2.1.3, Eplee and McClain 2000a, and Robinson and Wang 2000). This calibration is performed every time the level-2 processing algorithms are modified to ensure that the water-leaving radiances produced by the algorithms match the ground-truth measurements from MOBY. The vicarious calibration is also performed to include additional SeaWiFS and MOBY measurements taken over time.

3.3.1.4 Temperature Correction

A correction was made to the level-0 to -1 conversion software to correctly unpack the focal plane temperatures used in the calibration process. The effect of this correction on the water-leaving radiance values was less than 0.5% in bands 1–4, 1.5% in band 5, and 3.0% in band 6. Recalibration will remove most of these changes.

3.3.2 Atmospheric Correction Changes

A number of improvements were made in the algorithms that remove the radiance contributions of the atmosphere. As with the changes in the calibration (Sect. 3.3.1), some of the changes were made to correct artifacts seen in the data, and others were made to perform a more accurate atmospheric correction.

Table 2. Major changes in the third reprocessing.

Change	*Observable Effect*
Calibration:	
Expanded time-dependent calibration	Better temporal stability
Bilinear gain adjustments	Smooth transition to higher radiances
Revised vicarious calibration	None
Temperature correction	None
Atmospheric Correction:	
Modified aerosol model selection	Reduced discontinuity in some fields
Epsilon value extrapolation	Better retrieval of low chlorophyll values
Improved Rayleigh computation	Significant decrease in negative L_{WN} at high solar zenith angles
Pressure dependent transmittance	Small L_{WN} changes
Near-infrared L_{WN} adjustment	Significant decrease in negative L_{WN} and high chlorophyll values in coastal areas
Other:	
Modify C:K computation	Eliminate bad data values in binned data
Spectral-dependent whitecap correction	Small reductions in negative L_{WN} values
Sun glint correction	Greatly improved aerosol optical thickness
Ozone data interpolation	None
Improved $K(490)$ algorithm	Better $K(490)$ values in turbid water
Absorbing aerosol flagging	Reduce binning of contaminated data
Trichodesmium flagging	None
Improved chlorophyll algorithm	Slight lowering of low chlorophyll values
Out-of-band correction	Better compatibility to *in situ* measurements
Navigation Improvements	Improved location of data
Improved coastal data inclusion	More coastal retrievals
Structural:	
Product and flag updates	Better flag specificity
Level-2 program code changes	Greater flexibilty, faster updates

3.3.2.1 Modified Aerosol Model Selection

It was discovered that the aerosol radiance fields contained noticable discontinuities in open ocean areas. The discontinuities, which paralleled lines of constant scattering angle, propagated noticable and unwanted artifacts in the SeaWiFS products. The effect became more noticable after smoothing of the near-infrared radiance fields—a method under investigation for improving the data quality (e.g., to reduce speckling).

The discontinuity was caused by the transition between the oceanic aerosol model with 90% humidity and other models. This model was removed, leaving the oceanic aerosol model with 99% humidity to handle the very clear, oceanic aerosol conditions. To preserve the 12 model set, the coastal model with 70% humidity was reinstated to the model suite.

3.3.2.2 Epsilon Value Extrapolation

Even with the oceanic aerosol models that extend the coverage to a larger aerosol type range, there were many occasions when this range was exceeded. On these occasions, the ϵ value, which is an indicator of the aerosol type, has a value lower than that of the lowest aerosol model. In the second reprocessing, the ϵ value was used to interpolate between two aerosol models, or in the case of an ϵ value below the lowest model, it used the value of the lowest model instead of the true value. The result was the removal of more aerosol radiance than if the ϵ value could be extrapolated. The change made for the third reprocessing was to extrapolate the ϵ values for the other bands using an analytical function, so that a better aerosol correction could be made.

For test cases in open ocean areas where ϵ value extrapolation would occur, up to 24% of the L_{WN} retrievals benefitted from the extrapolation. No significant changes were observed in the chlorophyll fields, but the 412 nm water-leaving radiances were increased by an average of $0.1\,\mathrm{mW\,cm^{-2}\,sr^{-1}\,s^{-1}}$, an increase of about 6%.

3.3.2.3 Improved Rayleigh Computation

The Rayleigh radiance algorithm, which was used for the second reprocessing, contained no correction for ocean

surface roughness. The effect of ocean roughness is negligible at low and moderate solar zenith angles, but becomes significant at solar zenith angles greater than 60°. Without an adjustment for wind roughening, the Rayleigh radiance estimate is too high at high solar zenith angles and greater than zero wind speeds. This results in a reduction of the L_{WN} values and an increase in the occurrence of negative L_{WN} values. Tests of level-2 retrievals with the wind-dependent Rayleigh algorithm showed that negative water-leaving radiances were reduced in the 412 nm band from 80% to 40% at solar zenith angles of 70°, where the problem is most severe. The L_{WN} values at high solar zenith angles also increased significantly. The effects will be addressed further in Sect. 3.3.6.2.

3.3.2.4 Pressure Dependent Transmittance

Prior to the third reprocessing, the diffuse transmittance used in the computation of the normalized water-leaving radiance was derived from a look-up table with dependence only on the aerosol model and the viewing geometry. Now, a pressure correction (through the Rayleigh optical thickness) is also applied to both the sun-to-surface and surface-to-satellite diffuse transmittance (Wang 1999). The effect on L_{WN} values is small: a large change in the atmospheric pressure of 30 mbar causes about a 1% change in L_{WN} values at 412 nm while at 865 nm, the change is only 0.05%.

3.3.3 Near-Infrared L_{WN} Value Adjustment

One of the problems noted in the second reprocessing, which was examined closely in preparation for the third reprocessing, was the occurrence of negative water-leaving radiances in the SeaWiFS bands. It was apparent that especially in coastal regions, the water-leaving radiances in the 412 and 443 nm bands were negative for two reasons:

1. High chlorophyll content, which depressed the blue radiances, made water-leaving radiances near zero, and
2. Turbid coastal waters confuse the aerosol correction (absorbing aerosols could also be responsible), resulting in the overestimation of aerosol radiance, especially in the blue bands, thereby decreasing an already low radiance value, frequently causing it to become negative.

The negative water-leaving radiances are obviously unrealistic, although radiances approaching zero are common in turbid waters for bands 1 and 2. The negative L_{WN} values make the affected pixels useless for algorithms that rely on the blue bands as input. In the same regions having the negative L_{WN} problem, anomolously high chlorophyll was found, which again indicated that the blue bands were being excessively depressed.

The ocean science community responded to this problem with a number of algorithms to explain the problem and to get better L_{WN} estimates. The solutions fell into two categories:

1. The assumption of zero water-leaving radiance in the near-infrared bands at 765 and 865 nm is wrong in high chlorophyll or turbid waters. The algorithms attempt to use the chlorophyll values to estimate the water-leaving radiances in these bands; the algorithms were contributed by D. Siegel (Siegel et al. 2000), R. Arnone, and R. Stumpf.
2. After accounting for the near-infrared contribution, an assumption about the value of the 412 nm water-leaving radiance can be made so that it and the other L_W values do not become negative (R. Stumpf, pers. comm.).

The most promising combinations of these methods were tested, including the use of band 6 (instead of band 7) with band 8 in the aerosol determination. The methods were examined in detail for a number of test scenes that were affected by the problem. Also, the methods were tested in general on two 8 day periods of SeaWiFS GAC data—one in January 1998 and one in July 1998. The results were then compared to the method used in the second reprocessing. Although investigation of the other methods will continue, the Siegel method (Siegel et al. 2000) was chosen for the third reprocessing because of its simplicity and because it produced significant decreases in the amount of negative L_{WN} values and lowered the coastal chlorophyll values to more reasonable levels.

3.3.4 Other Changes

Several other changes were made in the level-2 and -3 processing in preparation for the third reprocessing. As a result of the level-2 data set format change (Sect. 3.3.5), two new flagging algorithms were added to indicate the presence of absorbing aerosols and *Trichodesmium*. Improvements were made to the chlorophyll, diffuse attenuation, ozone, and whitecap algorithms. A glint correction yielded better atmospheric optical depth and an out-of-band correction permitted better comparison of L_{WN} with *in situ* values.

3.3.4.1 Modified C_a:K Computation

After the second reprocessing was completed, it was discovered that some level-3 binned products had infinite values stored in some bins for the parameter containing the ratio of the chlorophyll *a* (C_a) values to the diffuse attenuation coefficient at 490 nm [$K(490)$]. The problem was introduced because of the new binning policy which allowed the binning of negative L_{WN} data, combined with some shortcomings in the binning code.

The $K(490)$ algorithm in the level-2 processing was set to return a zero value for $K(490)$ if either the L_{WN} at 490 or 555 nm was less than zero. When a $K(490)$ value of zero was used in the binner to produce C_a:K, a value of infinity

was assigned to that bin. This problem was compounded for products covering longer time periods because once a bin had an infinite value in it, no amount of averaging would lessen or remove it; therefore, eight day, monthly, and yearly binned products would accumulate more bins with infinite C_a:K values.

This problem was fixed in both the $K(490)$ algorithm in the level-2 code and in the C_a:K computation in the binner. In the $K(490)$ algorithm, the computation was modified so that zero $K(490)$ values would not be produced. The following rules were made to deal with the L_{WN} conditions:

a. If $L_{WN}(490)$ and $L_{WN}(555) > 0$, then compute $K(490)$ normally.
b. If $L_{WN}(490) < 0$, then set $K(490) = 6.4$.
c. If $L_{WN}(490) > 0$ but L_{WN} at 555 nm < 0, then set $K(490) = 0.016$.

The actions taken for zero L_{WN} values represent the maximum $K(490)$ value that can be stored in the level-2 data set and the lowest possible $K(490)$ value which the algorithm can produce. Tests with SeaWiFS data showed that these default values agreed well with the surrounding $K(490)$ values. The C_a:K algorithm in the binner was also adjusted to use a $K(490)$ value of 0.016 in the calculation if it encountered a zero value.

In addition, a modification was made in the masking conditions for the atmospheric failure so that fewer high $K(490)$ values erroneously derived over open ocean areas would be binned. If the L_W for any of the 490, 510, or 555 nm bands are less than zero, the atmospheric warning flag is set in the level-2 file and applied as a mask in the level-3 binning.

3.3.4.2 Changes to Whitecap Correction

For the third reprocessing, three changes were made in the whitecap correction. The first change was to use a correction with a spectral dependence (Frouin et al. 1996). The second change was to increase the strength of the correction by approximately 65% from the values used in the second reprocessing. The third change was to limit the whitecap correction for wind speeds above $8\,\mathrm{m\,s^{-1}}$ to the value found at $8\,\mathrm{m\,s^{-1}}$. This limit was set to avoid overcorrections for whitecaps. This strategy incorporated more recent information on whitecaps (Moore et al. 2000), yet avoided overcorrection at high wind speeds.

The effects on the radiances were small, but noticable. No significant change was observed for areas with wind speeds less than $10\,\mathrm{m\,s^{-1}}$. For areas with winds from 10–$15\,\mathrm{m\,s^{-1}}$, the occurrence of negative water-leaving radiance at 412 nm was reduced by 3%, and above $15\,\mathrm{m\,s^{-1}}$, negative L_{WN} values at 412 nm were reduced by 10%.

3.3.4.3 Sun Glint Correction

The SeaWiFS Project found that the aerosol optical thickness was noticably higher for areas surrounding the subsolar point. The atmospheric correction was accounting for glint outside the glint mask as additional aerosol radiance. This did not noticably affect the L_{WN} and chlorophyll retrievals, but it inflated the aerosol optical thickness, making it less useful. The level-2 processing program already calculated an estimate of the glint radiance, so the program was changed to remove the glint radiance outside the glint mask as a part of the processing. The glint removal was made more robust by performing a second iteration with a better value of the aerosol optical thickness. Details of the glint correction are found in Wang and Bailey (2000).

3.3.4.4 Ozone Data Interpolation

In previous reprocessings, the Total Ozone Mapping Spectrometer (TOMS) ozone values (the primary SeaWiFS ozone source) were interpolated to the time of the SeaWiFS data pass assuming that the TOMS data were all taken at 1200 UTC. In fact, the TOMS data were collected over the daylight side of the Earth from east to west with a phasing very close to SeaWiFS (the data were taken almost at the same time). The ancillary data selection and interpolation routines in the level-2 processing were modified to use this information to calculate ozone fields which would be more representative of the actual conditions at the time of the pass (Ainsworth and Patt 2000). The effect is the smallest around 1200 UTC, which is near the prime meridian, and the greatest near ±180° longitude.

3.3.4.5 Improved K(490) Algorithm

An improved $K(490)$ algorithm (Mueller 2000) was implemented for the third reprocessing. The previous algorithm used $L_W(443)$ and had errors in regions of highly turbid water and in bloom situations where $L_W(443)$ can be underestimated. The new algorithm estimates $K(490)$ by using the ratio $L_{WN}(490)$:$L_{WN}(555)$.

3.3.4.6 Absorbing Aerosol Flag

In many ocean regions, and especially off the west coast of Africa, absorbing aerosols (suspended dust) are not handled by the aerosol determination algorithm. Currently, the suite of aerosol models does not contain absorbing aerosol models. For the third reprocessing, an algorithm was implemented to detect significant amounts of absorbing aerosols (Hsu et al. 2000). A new level-2 flag was made to indicate measurements in regions of excessive absorbing aerosol. This flag is used to exclude data during the level-3 binning phase.

3.3.4.7 Trichodesmium *Flag*

An algorithm was implemented in the third reprocessing that detects the presence of *Trichodesmium* bloom conditions (Subramaniam et al. 2000). The existance of a

bloom is indicated by one of the new level-2 flags, which currently is not used for any level-3 exclusion.

3.3.4.8 Improved Chlorophyll a *Algorithm*

The chlorophyll algorithm used for the third reprocessing (OC4) (O'Reilly et al. 1998), was used in place on the OC2 algorithm (second reprocessing); a larger *in situ* data set was used to refine the OC4 algorithm (O'Reilly et al. 2000). The OC4 algorithm also has the property of not reporting negative chlorophyll values as the previous OC2 algorithm did. The range of chlorophyll in the output is expanded at the low end to include values from 0–0.009 mg m^{-3} in steps of 0.001. Previously, the lowest reported chlorophyll value was 0.01 mg m^{-3}. In general, the new algorithm was found to slightly reduce the chlorophyll in the range from 0.01–0.05 mg m^{-3}.

3.3.4.9 Out-of-Band Correction

The eight SeaWiFS bands have broad response functions compared to most instruments that measure L_W in the field. Although the processing of radiances to the water-leaving radiance includes the out-of-band response, the resulting L_W values retain the initial broad response function. For the third reprocessing, an out-of-band correction was applied to the L_W values as the default (Wang et al. 2000). The correction has the greatest effect at 555 nm where in low chlorophyll waters (high blue radiances), the corrected L_{WN} values can be 5–10% lower than the uncorrected values. The use of the out-of-band correction slightly decreased the chlorophyll values by about 15% in the range from .01–.05 mg m^{-3}.

3.3.4.10 Navigation Improvements

Improvements were made to the navigation algorithms in the level-0 to -1A software to reduce the seasonal variations in geolocation accuracy and to handle operational changes in the available navigation data from the satellite. These changes improved the overall navigation of the data.

3.3.4.11 Improved Coastal Data Inclusion

Some instances were observed when the radiance at 412 nm—after being corrected for Rayleigh, glint, ozone, and whitecaps—was negative for otherwise clear regions. This condition occurred infrequently along coastal areas, but affected significant regions in any one single data pass. The atmospheric failure masking used in the second reprocessing used this test to exclude observations that had these conditions in any of the eight SeaWiFS bands. In the third reprocessing, this exclusion was removed for the 412 nm band so more coastal areas could be processed. This change was observed to increase the number of retrievels at many coastal regions for approximately one out of every four passes.

3.3.5 Major Product and Flag Changes

Since the SeaWiFS launch, the Project has been creating the same suite of products and flags (McClain et al. 1995 and McClain 2000). With the third reprocessing, the Project took the opportunity to revise the product suite and to expand the flag set to respond to new demands.

Table 3. Operational products for the third reprocessing.

Product Name	*Description*
`nLw_412`	L_{WN} values at 412 nm
`nLw_443`	L_{WN} values at 443 nm
`nLw_490`	L_{WN} values at 490 nm
`nLw_510`	L_{WN} values at 510 nm
`nLw_555`	L_{WN} values at 555 nm
`nLw_670`	L_{WN} values at 670 nm
`angstrom_510`	Ångström coefficient at 510 and 865 nm
`chlor_a`	Chlorophyll *a* concentration
`K_490`	Diffuse attenuation coefficient at 490 nm
`eps_78`	Epsilon value at 765 and 865 nm
`tau_865`	Aerosol optical thickness at 865 nm

3.3.5.1 Product Suite Changes

Table 3 shows the operational product suite used in the third reprocessing and the product names used in SeaDAS. The CZCS pigment product (`CZCS_pigment`) was removed because there was little demand for it and because a simple equation can be used to derive the pigment from the chlorophyll product. Also, the two products of the aerosol radiance at 670 nm and at 865 nm (`La_670` and `La_865`) were removed in favor of the normalized water-leaving radiance at 670 nm (`nLw_670`). The Ångström coefficient at 510 nm (`angstrom_510`), was included because many researchers use the Ångström coefficient to characterize the aerosol type.

Similar changes were made in the level-3 binned products. In place of the `La_670` and `CZCS_pigment` are the `nLw_670` and `angstrom_510` products.

3.3.5.2 Flag Changes

For previous reprocessings, the suite of flags was limited to 16 by the format of the level-2 data set. In the third reprocessing, the available room for flags was expanded to 32, of which only 24 flags are currently defined. Table 4 lists these flags and their status as masks in excluding data in the level-2 and -3 operational products.

The original 16 flags have much the same meaning as before with some exceptions. In the second reprocessing, the atmospheric algorithm failure flag (`EPSILON1`) included many conditions that prevented the calculation of

Table 4. Flags for the third reprocessing. The "Flag Name" column denotes the flag names as of the third reprocessing, whereas the "Old Name" column is the flag name used in the second reprocessing. The "Mask In" columns indicate that no geophysical data is created in the level-2 (L2) or level-3 (L3) data set if the flag conditions marked "Y" exist for that observation.

Flag Number	*Flag Name*	*Mask In L2*	*Mask In L3*	*Old Name*	*Description*
1	ATMFAIL	Y	Y	EPSILON1	Atmospheric algorithm failure
2	LAND	Y	Y	LAND1	Land
3	BADANC			ANCIL1	Missing ancillary data
4	HIGLINT	Y	Y	SUNGLINT1	Sun glint contamination
5	HILT	Y	Y	HIGHLT1	Total radiance above the knee in any band
6	HISATZEN		Y	SATZEN1	Satellite zenith angle above the limit
7	COASTZ			COASTZ1	Shallow water
8	NEGLW			NEGLW1	Negative water-leaving radiance in any band
9	STRAYLIGHT		Y	STRAYLIGHT1	Stray light contamination
10	CLDICE	Y	Y	CLDICE1	Clouds or ice
11	COCCOLITH		Y	COCCOLITH1	Coccolithophore bloom
12	TURBIDW		Y	TURBIDW1	Turbid, Case-2 water
13	HISOLZEN		Y	SOLZEN1	Solar zenith angle above the limit
14	HITAU			HIGHTAU1	High aerosol concentration
15	LOWLW		Y	LOWLW1	Low water-leaving radiance at 555 nm
16	CHLFAIL	†	Y	CHLOR1	Chlorophyll not calculable
17	NAVWARN		Y		Questionable navigation (tilt change)
18	ABSAER		Y		Absorbing aerosol index above the threshold
19	TRICHO				*Trichodesmium* bloom condition
20	MAXAERITER		Y		Maximum number of iterations in the NIR algorithm
21	MODGLINT				Glint corrected measurement
22	CHLWARN				Chlorophyll is out of range
23	ATMWARN		Y		Epsilon value outside of reasonable range or L_W 510, at 490, or 555 nm is less than zero
24	DARKPIXEL				Rayleigh corrected radiance is less than zero for any band

† The chlorophyll value is not computed, but *first guess* L_{WN} values are computed.

the aerosol radiances and thus, the L_{WN} values. It also indicated times when the ϵ value was outside reasonable limits defined by the standard aerosol models; hence, the name EPSILON1. Now, the atmospheric algorithm failure flag (renamed to ATMFAIL), only indicates conditions where L_{WN} values could not be calculated. The new ATMWARN flag indicates when the ϵ value is outside the reasonable range but L_{WN} values could be calculated. It also indicates observations where L_W values in the 490, 510, and 555 nm bands are negative. A serious problem condition, when the Rayleigh corrected radiances are negative, is indicated in the new DARKPIXEL flag so that this condition can be monitored more easily. In the second reprocessing, the chlorophyll algorithm failure flag (CHLOR1) indicated both conditions where chlorophyll could not be computed and when chlorophyll exceeded the high threshold. Now, the CHLFAIL flag only indicates when chlorophyll can not be calculated, because the input L_{WN} values are less than zero, or when the calculated chlorophyll is outside physical limits (greater than $640\,\mathrm{mg\,m^{-3}}$). The new CHLWARN flag signals chlorophyll values which exceed the high value that can be stored in the product (greater than $64\,\mathrm{mg\,m^{-3}}$), or very small values (less than $0.01\,\mathrm{mg\,m^{-3}}$).

The remaining six new flags address new conditions or are used to more consistently handle current conditions. The NAVWARN flag is used primarily to indicate where less reliable navigation is expected, such as when the instrument tilt is changing. The level-3 binning can use the NAVWARN flag to decide on binning instead of having to use the tilt indicator in the level-2 data. The ABSAER and TRICHO flags indicate the existence of absorbing aerosols and *Trichodesmium* blooms detected by new algorithms. The MAXAERITER flag indicates when the NIR correction algorithm (Sect. 3.3.3) has been unable to converge on a NIR L_{WN} estimate. Finally, the MODGLINT flag indicates pixels where the glint correction was applied.

3.3.6 Third Reprocessing Analysis

The processing software for the third reprocessing was updated with all the changes mentioned in Sects. 3.3.1–

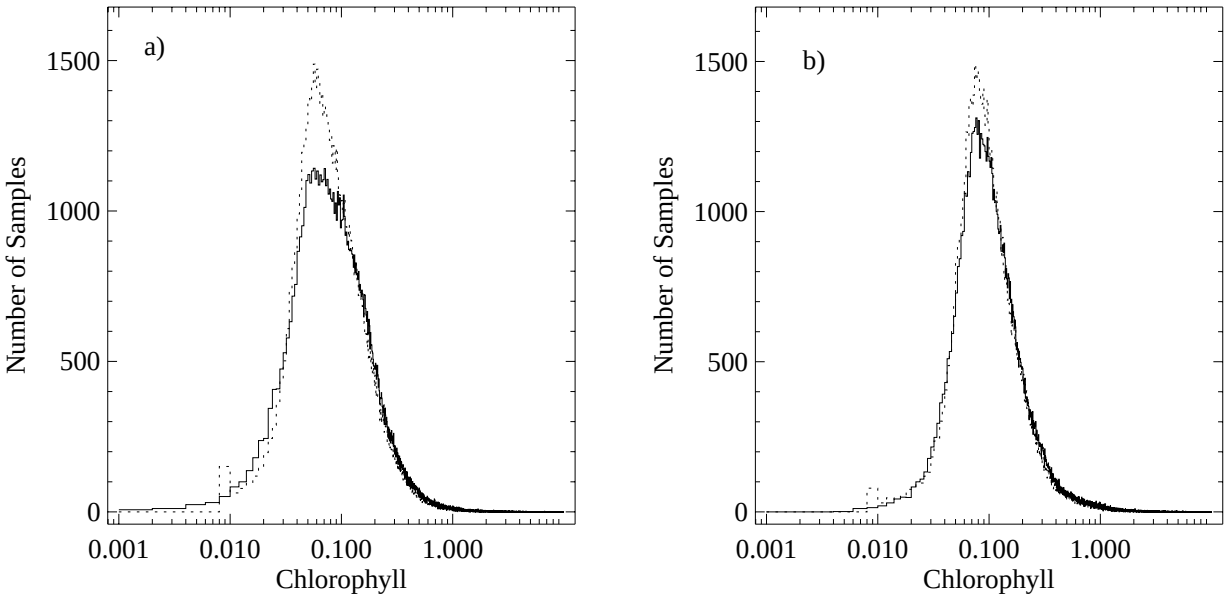

Fig. 3. The SeaWiFS level-3 global chlorophyll *a* frequency distribution for the eight day period of **a)** 17–24 January 1998, and **b)** 12–19 July 1998, made with the second reprocessing (dotted curve) and the third reprocessing (solid curve).

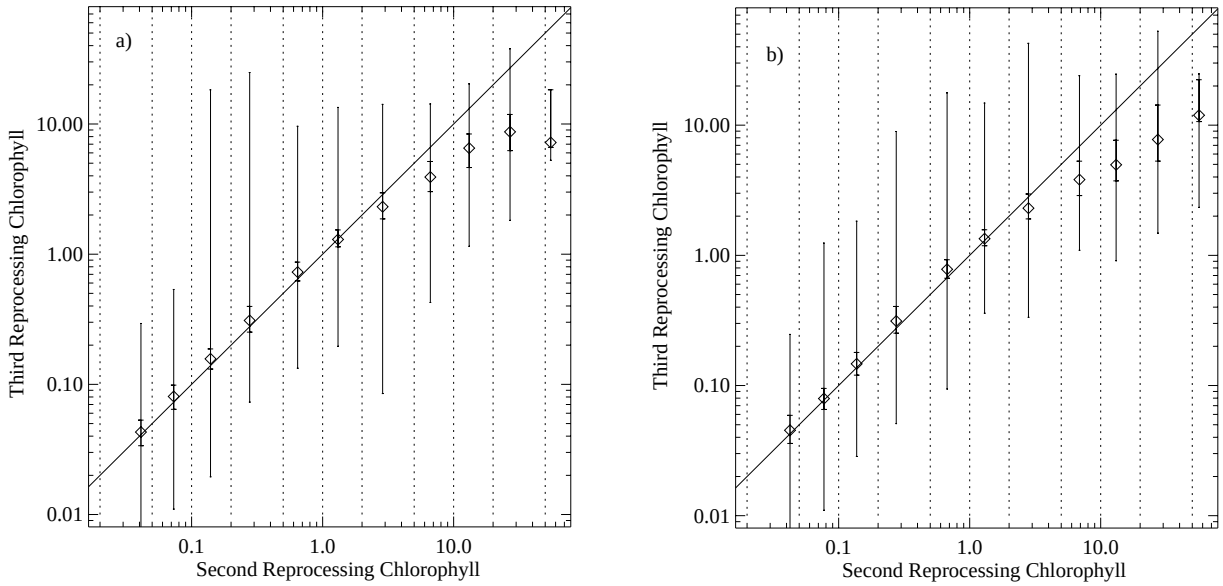

Fig. 4. Comparison of the chlorophyll retrieved in the third reprocessing (y axis) to that retrieved in the second reprocessing (x axis) for **a)** 17–24 January 1998, and **b)** 12–19 July 1998. For level-3 binned chlorophyll from the second reprocessing in 11 ranges from 0.02–64.0 $\mathrm{mg\,m^{-3}}$, the median third reprocessing chlorophyll value is plotted as diamonds. The nearest set of bars is the range of data in the second-to-third quartiles, while the outer bars show the extreme range of the third reprocessing chlorophyll values. Chlorophyll values greater than 2 $\mathrm{mg\,m^{-3}}$ were significantly reduced in the third reprocessing.

3.3.5. The vicarious calibration for bands 1–7 was performed with the new algorithms. The new algorithms and the new calibration were used to process two eight day periods in January (17–24 January 1998) and July (12–19 July 1998). The results of these runs, in comparison to the second reprocessing runs, will be discussed next.

3.3.6.1 Chlorophyll a

Figure 3 is a plot of the global distribution of chlorophyll for the January and July periods. The inclusion of binned chlorophyll in the 0–0.009 mg m^{-3} range for the third reprocessing can be seen, as can the artificial pile-up of values, at 0.01 mg m^{-3}, for the second reprocessing. The third reprocessing produced a greater number of chlorophyll values in the 0–0.04 mg m^{-3} range than the second reprocessing, which indicates that the chlorophyll values in this range are reduced. For a test area in the Pacific (around 12°N, 135°E), located in one of the lowest chlorophyll areas in the data, the average chlorophyll value dropped from 0.057–0.0381 mg m^{-3}, a 34% decrease. In the chlorophyll range above 0.07, the third reprocessing increased the chlorophyll values. The magnitude of the changes in July period are less, but still follow the same trend.

Figure 4 shows the change that occurred in chlorophyll more clearly for the middle and high range chlorophyll. Figure 4 summarizes a scatterplot comparing binned chlorophyll from the third reprocessing versus the second reprocessing. For a number of chlorophyll ranges in the second reprocessing data, the statistics of the matching the third reprocessing chlorophyll values are plotted. The median is indicated by the diamond, and the inner quartiles are the inner bounding ticks on the vertical bar. In the 0.2–1.0 mg m^{-3} range, the third reprocessing shows a slight increase in the chlorophyll value of about 10%, as was seen in the histograms (Fig. 3). For chlorophyll values greater than 2 mg m^{-3}, the third reprocessing significantly lowered the chlorophyll value. In the 5–10 mg m^{-3} range, the third reprocessing lowered the chlorophyll values by about 40%, and lowers it even more for higher values. This lowering of high chlorophyll is primarily due to the Siegel NIR algorithm and greatly reduces chlorophyll values in all the coastal and upwelling regions.

To illustrate how the third reprocessing methodology improves chlorophyll *a* retrievals in coastal waters, SeaWiFS chlorophyll values were compared with *in situ* pigment data from the Chesapeake Bay in the US. Three time periods in 1998 were selected for this analysis: 11–19 April, 4–12 August, and 19–23 October. For each time period, HRPT data were processed to level-2 chlorophyll using both the second and third reprocessings and methodologies and were then space- and time-binned. *In situ* data (originally provided by L. Harding, University of Maryland), were obtained from the SeaWiFS Bio-optical Archive and Storage System (SeaBASS). Only the lower Chesapeake Bay, south of 38.5°N latitude, was considered in this analysis. For all three time periods, the mean SeaWiFS-retrieved chlorophyll value exceeds that of the mean *in situ* value. The third reprocessing values, however, are 62.5, 57.3, and 52.8% lower than the second reprocessing values, for April, August, and October, respectively (Table 5). Additionally, the ratio of mean SeaWiFS, to mean *in situ* chlorophyll values is reduced from 3.57–1.34 for April, 2.39–1.02 for August, and 2.27–1.07 for October. Results from these comparisons (especially the latter) indicate that the methodology for the third reprocessing significantly improves SeaWiFS chlorophyll *a* retrievals in coastal regions. The number of successful chlorophyll retrievals also increased by more than 10% for two of the three time periods.

3.3.6.2 Negative L_{WN} Values

The use of the Siegel NIR algorithm, and the wind speed correction to the Rayleigh radiance algorithm (Sect. 3.3.2.3) have both significantly helped in the reduction of negative L_{WN} values globally. In the January time period, the number of negative L_{WN} values in the binned data for the 412 nm band was reduced from 2.5–2.1% of the total, while in the July time period, the reduction was from 5.2–4.7%. Figure 5 shows the geographical regions, in the July time period, where the percentage of negative L_{WN} values are higher than 50% for the third reprocessing. Compared with the same display for the second reprocessing (Fig. 2), the reduction of negative L_{WN} values at high solar zenith angles, and especially in the Southern Ocean, is dramatic. The improved performance of the atmospheric correction with the wind dependent Rayleigh radiances is the main reason why the useful solar zenith limit for data was increased from 70–75°. Slight reductions can also be seen in the occurrence of negative L_{WN} along coastal areas.

The impact on negative L_{WN} values of the wind speed correction to the Rayleigh radiances is illustrated in Fig. 6, which shows the percentage of negative L_{WN} as a function of solar zenith angle for 412, 490, and 555 nm SeaWiFS bands in the July time period (the other bands and the January time period show similar behavior). In the 412 nm band, at solar zenith angles from 65–70°, the percentage of measurements with negative L_{WN} values dropped from 60% to 20%, with similar decreases in the other bands.

Figure 7 shows the mean of the L_{WN} values as a function of solar zenith angle for the same SeaWiFS bands in the July time period. The decrease in the mean L_{WN}, which begins at solar zenith angles of about 60°, could lower the L_{WN} values in the 412 nm band to less than zero in the second reprocessing (Fig. 7a). In addition, the 555 nm band average (Fig. 7c) dropped below 0.15, a masking threshold for removing data contaminated by cloud shadows. The third reprocessing significantly increases these means at high solar zenith angles and greatly reduces the aforementioned problems in the 412 and 555 nm bands, as well as increasing L_{WN} values in the other bands

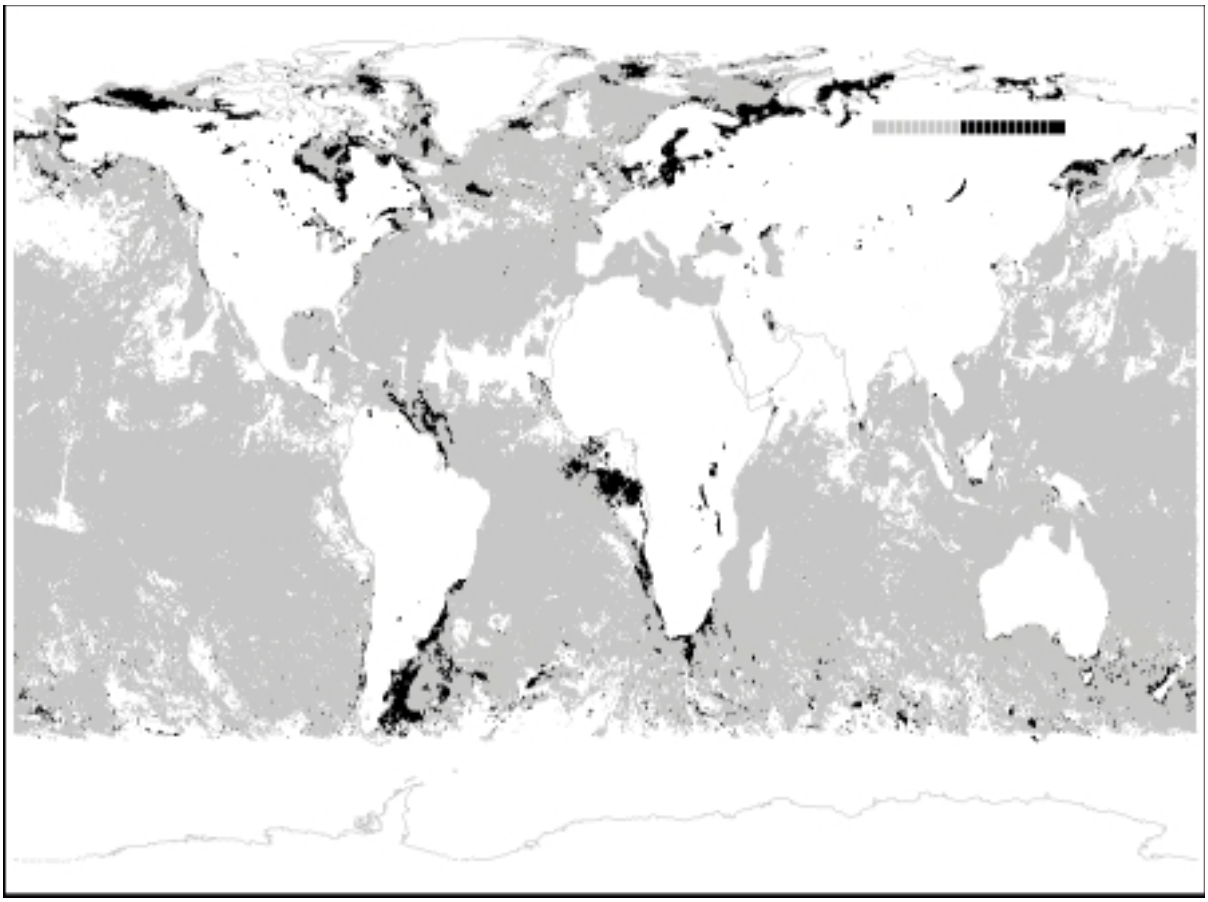

Fig. 5. Percentage of occurrence of negative L_{WN} values at 412 nm for the eight day period from 12–19 July 1998. This image was generated using the third reprocessing algorithms and uses data that is excluded by the standard level-2 processing: atmospheric correction algorithm failure, land, sun glint, high total radiance, and clouds. In addition, stray light pixels are excluded. White areas indicate no data—continental land masses make up a great part of this region—while light gray indicates data present with occurrences of negative L_{WN} values of less than 50%. The regions shaded black all have more than 50% occurrence of negative L_{WN} values, indicating areas that are severely affected by negative L_{WN}. In regions where the solar zenith angle is high, such as the Southern Ocean and along the coast, the amount of negative L_{WN} values were reduced relative to the second reprocessing (Fig. 2).

Table 5. Average chlorophyll in the Chesapeake Bay derived from *in situ* measurements (SeaWiFS second and third data reprocessings). The mean chlorophyll *a* values ($\bar{x}$) are in milligrams per cubic meter ($\mathrm{mg\,m^{-3}}$). The standard deviation (σ) and number of observations are also given.

Date	*In Situ*			*Second Reprocessing*			*Third Reprocessing*		
	$\bar{x}$	σ	*Obs.*	$\bar{x}$	σ	*Obs.*	$\bar{x}$	σ	*Obs.*
11–19 April 1998	11.93	11.31	91	42.64	18.42	1755	16.01	7.96	1960
4–12 August 1998	10.83	10.61	89	25.93	13.93	1804	11.06	3.71	1810
19–23 October 1998	7.43	4.08	67	16.85	9.76	1815	7.96	2.97	2133

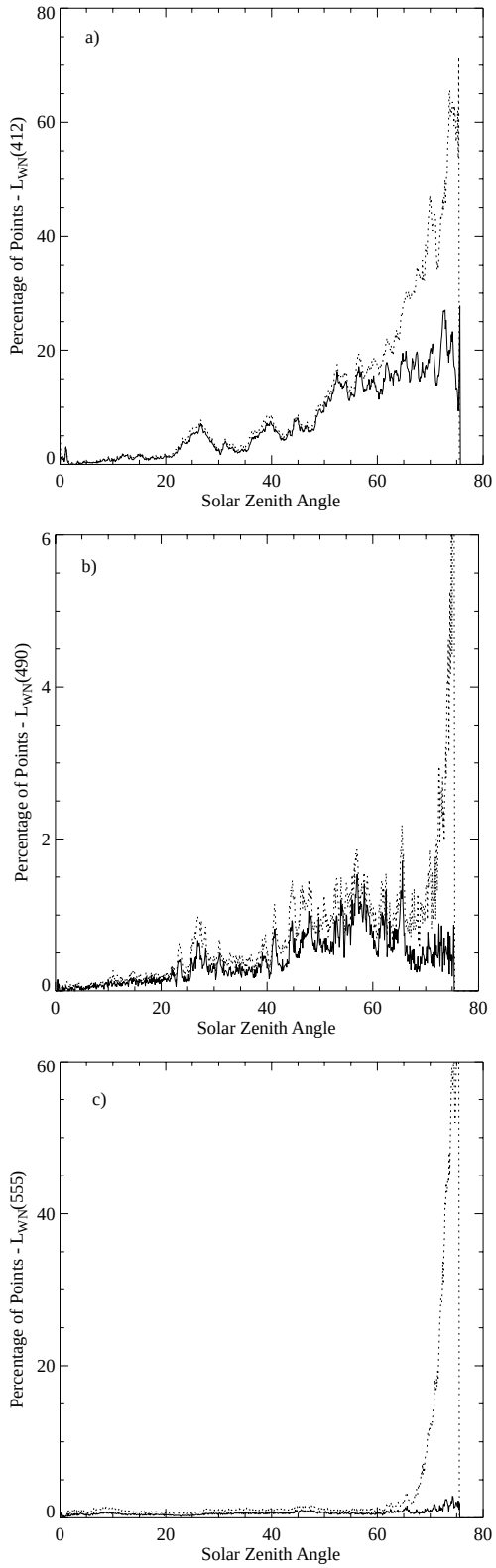

Fig. 6. Percentage of negative L_{WN} values as a function of the solar zenith angle for the eight day period of 12–19 July 1998 for the second (dotted curves) and third (solid curves) reprocessings. The SeaWiFS bands at **a)** 412, **b)** 490, and **c)** 555 nm are shown.

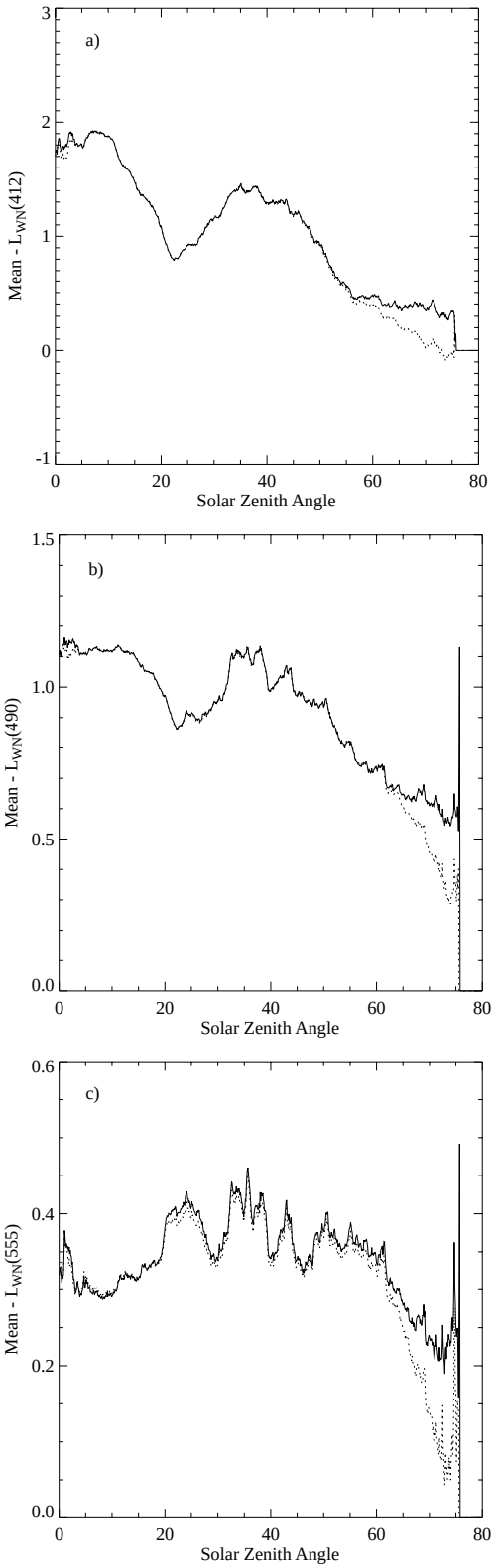

Fig. 7. Mean L_{WN} values as a function of solar zenith angle for the eight day period of 12–19 July 1998 for the second (dotted curves) and third (solid curves) reprocessings. The SeaWiFS bands at **a)** 412, **b)** 490, and **c)** 555 nm are shown.

and restoring a more constant value of L_{WN} in the green bands (510 and 555 nm).

In general, the number of level-3 bins filled in the eight day time bins of the third reprocessing increased over those in the second reprocessing by 1.2% and 2.4% for the January and July test periods. This corresponds to an increase in ocean coverage of 1.8×10^6 and $3.8\times10^6\,\mathrm{km}^2$. Much of this increase is due to the improved, wind-dependent Rayleigh radiance algorithm and the opening of the solar zenith angle cutoff for binning from 70–75°.

More results of the quality of the SeaWiFS L_{WN} values and chlorophyll can be found in Bailey et al. (2000). These comparisons show marked improvement in the L_{WN} and chlorophyll values compared to *in situ* measurements.

3.4 CONCLUSION

The second reprocessing repaired many large problems and, for the most part, brought about favorable changes in both the chlorophyll and L_{WN} distributions. The changes increased very low chlorophyll values in open-ocean regions, and decreased the values of high chlorophyll greater than $1.0\,\mathrm{mg\,m}^{-3}$ and in many cases, allowed more chlorophyll retrievals to be made and binned in the level-3 data. L_{WN} values generally increased although the prevelance of negative L_{WN} was recognized as a major problem remaining. Negative L_{WN} values were found to be most prevelant in bands 1 and 2, at higher solar zenith angles, and around coastal areas where turbid, high chlorophyll concentrations exist.

The third reprocessing increased the usefulness of SeaWiFS data in both oceanographic and atmospheric applications. The negative L_{WN} problem, which was recognized and characterized in the second reprocessing, was addressed and significantly reduced in the third reprocessing using a correction of the near-infrared L_{WN} values and a wind-dependent correction to the Rayleigh radiance calculation. Abnormally high coastal chlorophyll values were decreased, and data at higher solar zenith angles were retrieved, as a result of these improvements. A chlorophyll algorithm that benefits from an increased observation set improved the retrieval of chlorophyll from the L_{WN} data. These and many other changes combined to improve the agreement of SeaWiFS L_{WN}, chlorophyll, and aerosol optical thickness to *in situ* observations.

In summary, the changes made for the second and third reprocessings have been wide ranging and have had a positive influence on all of the SeaWiFS products. Even so, there are many more possible improvements in future reprocessings that will be explored. The occurrence of negative L_{WN} values, although reduced, is still a problem in the coastal regions. More work is planned to improve the NIR methods and possibly include absorbing aerosols in the aerosol model suite. Work is under way to improve the cloud detection and masking algorithm. Other algorithms will be examined and improved, such as the algorithm for the turbid water flag.

References

Ainsworth, E.J., and F.S. Patt, 2000: "Modifications to the TOMS Ozone Ancillary Data Interpolation." In: McClain, C.R., E.J. Ainsworth, R.A. Barnes, R.E. Eplee, Jr., F.S. Patt, W.D. Robinson, M. Wang, and S.W. Bailey, SeaWiFS Postlaunch Calibration and Validation Analyses, Part 1. *NASA Tech. Memo. 2000–206892, Vol. 9,* S.B. Hooker and E.R. Firestone, Eds., NASA Goddard Space Flight Center, ???–???.

Bailey, S., et al, 2000: L_{WN} and chlorophyll matchup analysis, TM, Vol 10, ch ???.

Ding, K., and H.R. Gordon, 1994: Atmospheric correction of ocean-color sensors: effects of the Earth's curvature., Appl. Opt., 33, 7096 - 7106.

Eplee, R.E., Jr., 2000: "Calibration 'Knee' Offset Adjustments." In: McClain, C.R., E.J. Ainsworth, R.A. Barnes, R.E. Eplee, Jr., F.S. Patt, W.D. Robinson, M. Wang, and S.W. Bailey, SeaWiFS Postlaunch Calibration and Validation Analyses, Part 1. *NASA Tech. Memo. 2000–206892, Vol. 9,* S.B. Hooker and E.R. Firestone, Eds., NASA Goddard Space Flight Center, ???–???.

Eplee, R.E., Jr., and R.A. Barnes, 2000a: "Lunar Data Analyses for SeaWiFS Calibration." In: McClain, C.R., E.J. Ainsworth, R.A. Barnes, R.E. Eplee, Jr., F.S. Patt, W.D. Robinson, M. Wang, and S.W. Bailey, SeaWiFS Postlaunch Calibration and Validation Analyses, Part 1. *NASA Tech. Memo. 2000–206892, Vol. 9,* S.B. Hooker and E.R. Firestone, Eds., NASA Goddard Space Flight Center, ???–???.

Eplee, R.E., Jr., and R.A. Barnes, 2000b: "Solar Data Analyses for SeaWiFS Calibration." In: McClain, C.R., E.J. Ainsworth, R.A. Barnes, R.E. Eplee, Jr., F.S. Patt, W.D. Robinson, M. Wang, and S.W. Bailey, SeaWiFS Postlaunch Calibration and Validation Analyses, Part 1. *NASA Tech. Memo. 2000–206892, Vol. 9,* S.B. Hooker and E.R. Firestone, Eds., NASA Goddard Space Flight Center, ???–???.

Eplee, R.E., Jr., and C.R. McClain, 2000a: "MOBY data analysis for vicarious calibration of SeaWiFS." In: McClain, C.R., E.J. Ainsworth, R.A. Barnes, R.E. Eplee, Jr., F.S. Patt, W.D. Robinson, M. Wang, and S.W. Bailey, SeaWiFS Postlaunch Calibration and Validation Analyses, Part 1. *NASA Tech. Memo. 2000–206892, Vol. 9,* S.B. Hooker and E.R. Firestone, Eds., NASA Goddard Space Flight Center, ???–???.

Eplee, R.E., Jr., and C.R. McClain, 2000b: Global clear water analysis, TM 10, ch 7.???

Frouin, R., M. Schwindling, and P.-Y. Deschamps, 1996: Spectral reflectance of sea foam in the visible and near-infrared: *in situ* measurements and remote sensing implications. J. Geophys. Res., 101, 14,361-14,371.

Fukushima, H., M. Schmidt, B.J. Sohn, M. Toratani, and I. Uno, 1999: Detection of dust loaded airmass in SeaWiFS Imagery: an empirical dust index in comparison with model-predicted dust distribution over the Pacific in April 1998, Proc. of Int. Symp. on Remote Sens. '99, Korean Society of Remote Sensing, ISSN 1226-9743, pp. 89-94.

Gordon, H.R., and M. Wang, 1994: Influence of oceanic whitecaps on atmospheric correction of ocean color sensors. Appl. Opt., 33, 7354–7763.

Hsu, C., W.D. Robinson, S.W. Bailey, and P.J. Werdell, 2000: Absorbing Aerosol Index Description, TM 10, ch 1.

Johnson, B.C., E.E. Early, R.E. Eplee, Jr., R.A. Barnes, and R.T. Caffery, 1999: The 1997 Prelaunch Radiometric Calibration of SeaWiFS, SeaWiFS Postlaunch TM Vol 4.

Maritorena, S., and J.E. O'Reilly, 2000: Update on the Operational SeaWiFS Chlorophyll-a algorithm, TM 11 ch 1 ???

McClain, C.R., 2000: "SeaWiFS Postlaunch Calibration and Validation Overview." In: McClain, C.R., E.J. Ainsworth, R.A. Barnes, R.E. Eplee, Jr., F.S. Patt, W.D. Robinson, M. Wang, and S.W. Bailey, SeaWiFS Postlaunch Calibration and Validation Analyses, Part 1. *NASA Tech. Memo. 2000–206892, Vol. 9,* S.B. Hooker and E.R. Firestone, Eds., NASA Goddard Space Flight Center, ???–???.

McClain, C.R., R. Evans, J. Brown, and M. Darzi, 1995: "SeaWiFS Quality Control Masks and Flags: Initial Algorithms and Implementation Strategy," In: McClain, C.R., W.E. Esias, M. Darzi, F.S. Patt, R.H. Evans, J.W. Brown, K.R. Arrigo, C.W. Brown, R.A. Barnes, and L. Kumar: SeaWiFS Algorithms, Part 1. NASA Tech. Memo. 104566, Vol 28, S.B. Hooker, E.R. Firestone, and J.G. Acker, Eds., NASA Goddard Space Flight Center, Greenbelt, Maryland, 3-7.

Moore, K.D., K.J. Voss, and H.R. Gordon, 2000: Spectral reflectance of whitecaps: Their contribution to water-leaving radiance., J. Geophys. Res., 105, 6493-6499.

Mueller J.L., 2000: K(490) algorithm update. TM 11 ch ???

O'Reilly, J.E., S. Maritorena, B.G. Mitchell, D.A. Siegel, K.L. Carder, S.A. Garver, M. Kahru, C. McClain, 1998: Ocean color chlorophyll algorithms for SeaWiFS, J. Geophys. Res., 103, 24,937-24,953.

O'Reilly et. al., 2000: New Chlorophyll-a algorithm. TM 11 ch ???.

Robinson, W.D., and M. Wang, 2000: "Vicarious calibration of SeaWiFS band 7." In: McClain, C.R., E.J. Ainsworth, R.A. Barnes, R.E. Eplee, Jr., F.S. Patt, W.D. Robinson, M. Wang, and S.W. Bailey, SeaWiFS Postlaunch Calibration and Validation Analyses, Part 1. *NASA Tech. Memo. 2000–206892, Vol. 9,* S.B. Hooker and E.R. Firestone, Eds., NASA Goddard Space Flight Center, ???–???.

Siegel, D.A., M. Wang, S. Maritorena, and W.D. Robinson, 2000: Atmospheric Correction of Satellite Color Imagery: The Black Pixel Assumption, Appl. Opt. (in press). ???

Subramaniam, A., R.R. Hood, C.W. Brown, E.J. Carpenter, and D.G. Capone, 2000: A Classification Algorithm For Mapping Trichodesmium Blooms Using SeaWiFS. Deep Sea Research, (submitted).

Wang, M., 1999: A Sensitivity Study of the SeaWiFS Atmospheric Correction Algorithm: Effects of Spectral Band Variations. Remote Sens. Environ. 67:348-359.

Wang, M., 2000: "Atmospheric correction algorithm updates." In: McClain, C.R., E.J. Ainsworth, R.A. Barnes, R.E. Eplee, Jr., F.S. Patt, W.D. Robinson, M. Wang, and S.W. Bailey, SeaWiFS Postlaunch Calibration and Validation Analyses, Part 1. *NASA Tech. Memo. 2000–206892, Vol. 9,* S.B. Hooker and E.R. Firestone, Eds., NASA Goddard Space Flight Center, ???–???.

Wang, M., and S.W. Bailey, 2000: Correction of the sun glint contamination on the SeaWiFS aerosol optical thickness retrievals." In: McClain, C.R., E.J. Ainsworth, R.A. Barnes, R.E. Eplee, Jr., F.S. Patt, W.D. Robinson, M. Wang, and S.W. Bailey, SeaWiFS Postlaunch Calibration and Validation Analyses, Part 1. *NASA Tech. Memo. 2000–206892, Vol. 9,* S.B. Hooker and E.R. Firestone, Eds., NASA Goddard Space Flight Center, ???–???.

Wang, M., B.A. Franz, and R.A. Barnes, 2000: "Analysis of SeaWiFS Spectral Bandpass Effects." TM 10, ch 2.